Article

Comparative Transcriptomic Analysis of Head in *Laodelphax striatellus* upon Rice Stripe Virus Infection

Youxin Yu [1,†], Yuanyuan Zhang [1,†], Mingshi Qian [1], Qiuxin Zhang [1], Guoqing Yang [1,2,3] and Gang Xu [1,2,3,*]

1   College of Plant Protection, Yangzhou University, Yangzhou 225009, China
2   Jiangsu Co-Innovation Center for Modern Production Technology of Grain Crops, Yangzhou University, Yangzhou 225009, China
3   Joint International Research Laboratory of Agriculture and Agri-Product Safety, the Ministry of Education of China, Yangzhou University, Yangzhou 225009, China
*   Correspondence: xugang@yzu.edu.cn
†   These authors contributed equally to this work.

Abstract: Rice stripe virus (RSV) is transmitted by the small brown planthopper (SBPH), *Laodelphax striatellus*, in a circulative-propagative manner. Multiple studies have proved that RSV can manipulate vector insects to facilitate its transmission and can alter the gene expressions in viruliferous SBPH. However, to the best of our knowledge, nobody has investigated the gene expressions in the head of SBPH after RSV acquisition. In this study, to investigate the genes and gene functions regulated by RSV infection in the head of SBPH, we used RNA sequencing to compare the transcriptional profiles between SBPH head samples that acquired RSV or not. Compared with the non-viruliferous SBPH, a total of 336 differentially expressed genes (DEGs) were identified in the head samples of viruliferous SBPH groups, including 186 up-regulated and 150 down-regulated genes. Here, we focused on DEGs that may be involved in RSV replication or transmission, primarily genes associated with the nervous system, cytochrome P450s, sugar metabolism, the olfactory system, and cuticular process, as well as genes that have been previously reported to affect virus transmission in insect vectors including ubiquitin-protein ligase (*E3*), ecdysone response gene (*E74A*), and vitellogenin receptor (*VgR*). Finally, we verified the accuracy of the transcriptome sequencing results using qRT-PCR by selecting 16 DEGs. Our results can contribute to the understanding of the effects of RSV infection on gene regulation in the head of SBPH and provide insight into the control of plant virus transmission and insect vectors.

Keywords: *Laodelphax striatellus*; rice stripe virus; transcriptomic analysis; virus replication; neural associated genes

1. Introduction

Plant viruses induce the second highest number of plant diseases, causing tremendous economic losses to crops yearly, most of which can be transmitted by Hemipteran insects including planthoppers, whiteflies, leafhoppers, thrips, and aphids [1–5]. The spread of insect-vectored plant viruses in the field is mediated by complex interactions among virus–host–insect vectors [6–8]. These interactions have been fine-tuned by evolutionary forces, resulting in some instances where viruses can directly or indirectly manipulate arthropods with profound implications for virus spread and dispersal [6,7,9]. Most of the viral manipulation of vectors is characterized by indirect manipulation through alterations to the host plants, as seen with the cucumber mosaic virus (CMV) and Potato leafroll virus (PLV) [6,10]. In addition, vector-borne viruses could manipulate vector behavior by directly affecting their olfactory and nervous systems [11]. For instance, tomato chlorosis virus (TCV) and southern rice black-streaked dwarf virus (SRBDV) regulated the expression of the olfactory-related genes of *Bemisia tabaci* and *Sogatella furcifera*, respectively, to mediate insect host preference and promote virus transmission [12,13]. Tomato yellow leaf curl virus (TYLCV) causes neurodegeneration by inducing brain apoptosis, resulting in the

dysfunction of the nervous system, and impairing the host preference of *B. tabaci*, thereby promoting the spread of the virus [11].

Rice stripe virus (RSV) is a typical member of the genus *Tenuivirus*, which is the causal agent of rice stripe, a devastating disease of rice production in East Asia. It is transmitted by the small brown planthopper (SBPH), *Laodelphax striatellus* (Hemiptera, Delphacidae), in a persistent and circulative-propagative manner [14–16]. RSV is ingested with plant sap via feeding by the SBPH; upon ingestion, the virus initially replicates and proliferates in the midgut epithelial cells, then after passing through the basal lamina barrier via the hemolymph, virus particles spread to other tissues and organs including the salivary glands [17,18]. After accumulating in the salivary glands, virus particles are ingested into healthy plants by viruliferous SBPH along with saliva, thus completing the horizontal transmission. The RSV virus particles that spread to the vicinity of the ovary bind to the vitellogenin (Vg) in the hemolymph and are transported to the ovarian reproductive area through the endocytosis mediated by the Vg receptor (VgR), finally entering the oocyte with the nutrient filaments and passing through the maternal generation to their offspring, thus completing vertical transmission [19,20]. Taken together, being both a host and vector for RSV, SBPH is very pivotal for its transmission in the landscape. Therefore, clarification of the molecular processes behind the ability of RSV to transport and replicate in SBPH will be beneficial to elucidate the interactions of RSV with its vector. Recent studies indicated that RSV could cross the salivary gland or midgut barrier by interacting with α-tubulin, importin α_2, and sugar transporter 6 (ST6), thereby enhancing the horizontal transmission of the virus in SBPHs [21–23]. The interaction of RSV with cuticular protein CPR1 and 26S proteasome allows it to evade the SBPH immune responses [24,25]. In addition, c-Jun N-terminal kinase JNK, ubiquitin-conjugating enzyme E2, nuclear receptor E75, ribosomal protein RPL18, decay protein ZFP36L1, autophagy-related gene Atg8, heat-shock cognate protein HSC70, and the co-chaperone of Hsp70 GrpE of SBPH have been demonstrated to be involved in the regulation of RSV replication and accumulation in SBPHs [26–33].

With the rapid development of RNA-Seq technology, transcriptome analysis has been widely used to explore the effects of external factors on insects [34–39]. In recent years, exploring the complex interaction between plant viruses and insect vectors at the transcriptional level has also become a research focus. In SBPHs, Zhang et al. [35] and Lee et al. [36] analyzed the total mRNA gene changes after RSV infection using transcriptome sequencing, while Zhao et al. [37] and Huang et al. [30] investigated the effects of RSV on the hemolymph and fat body using transcriptome sequencing. In addition, the effects of RSV infection on the olfactory system were elucidated using the genome data of SBPHs [40] and a comparative transcriptome analysis of the chemoreception organs [41]. Nevertheless, the response of SBPH heads, especially regarding neural-related genes, to RSV infection has not been explored. Thus, the comparative transcriptome analysis of heads (without antennae) from viruliferous and non-viruliferous SBPHs was performed. In this study, the differentially expressed genes (DEGs) possibly involved in the regulation of RSV infection or replication were classified, and then pathway enrichment analysis was performed. The DEGs potentially involved in RSV infection were verified using qRT-PCR. This study is expected to investigate the changes in candidate genes in the SBPH head, particularly neural genes whose altered expressions can modulate vector behavior, which, in turn, can have a significant impact on RSV transmission.

2. Materials and Methods

2.1. Insects

The SBPH strains were continuously reared on rice plants (Wuyujing 3, provided by China National Rice Research Institute, Hangzhou, China) at $26 \pm 1\ ^\circ$C, $80 \pm 5\%$ relative humidity, with a 16L:8D photoperiod in the laboratory, and the original strains were collected from infected rice fields in Yangzhou, Jiangsu Province, China [18,42,43]. In order to distinguish RSV-viruliferous and non-viruliferous SBPH, an individual female adult was detected via a dot immunobinding assay (DIBA) [44]. The offspring of the female infected

with RSV were regarded as viruliferous SBPHs. Similarly, the offspring of the female that was not infected with RSV were regarded as non-viruliferous SBPHs. In addition, RSV screening was carried out every month to ensure that the RSV-carrying frequency of viruliferous SBPH was maintained above 80%.

2.2. Samples Preparation

In this study, three-days-old SBPH adults were unified for our preparation of SBPH head samples. In order to obtain the heads of viruliferous SBPHs, we dissected the heads (without antennae) under a light microscopy, and then placed the rest of the body in another tube for DIBA [44]. After detection, the corresponding head of the body that carried RSV was picked out, and 100 heads (female-male ratio: 1:1) were selected as one sample of viruliferous SBPHs. The heads of non-viruliferous SBPHs were collected using similar methods. These SBPHs were originated from the same population. Three biological replicates were performed, and samples were stored at −80 °C until RNA isolation.

2.3. RNA Isolation and cDNA Library Construction for Sequencing

The total RNA from the heads of viruliferous and non-viruliferous SBPHs was extracted with TRIzol reagent (Invitrogen, Waltham, MA, USA) following the manufacturer's instructions. Agarose gel electrophoresis was used to monitor the degree of degradation and the contamination of the RNA. Then, the purity and the integrity of the RNA were tested using a NanoDrop 2000 spectrophotometer (Thermo Fisher, Waltham, MA, USA) and an RNA Nano 6000 Assay Kit of the Bioanalyzer 2100 system (Agilent Technologies, Palo Alto, CA, USA), respectively. The NEBNext® Ultra™ RNA Library Prep Kit for Illumina® (NEB, Ipswich, MA, USA) was used to build the cDNA libraries according to the NEB general library building method. After the libraries were qualified, Illumina sequencing was performed with the Illumina Novaseq 6000 platform (Illumina, San Diego, CA, USA). The cDNA library construction and transcriptome sequencing were completed by Novogene (Beijing, China).

2.4. Data Quality Controlling and Mapping to Reference Genome

After Illumina sequencing, we first performed a sequencing error rate check on the sequencing results, as the sequencing process itself is subject to machine error, and the sequencing error rate distribution check reflects the quality of the sequencing data. Subsequently, adapters, low-quality sequences, and sequences containing poly-N were removed. Simultaneously, the Q20 (percentage of bases with Phred values greater than 20 in total bases), Q30 (percentage of bases with Phred values greater than 30 in total bases), and GC (guanine-cytosine) content of the clean reads were calculated. After filtering the raw reads, checking the sequencing error rate, and checking the GC content distribution, the clean reads were obtained and used for all downstream analyses. All clean reads were aligned to the SBPH reference genome [40] using HISAT2 v2.0.5 (http://www.ccb.jhu.edu/software/hisat (accessed on 27 July 2022)). All raw transcriptome data have been submitted to the National Center for Biotechnology Information SRA database (PRJNA884194).

2.5. Analysis of Differentially Expressed Genes and Enrichment

The analysis of the differentially expressed genes (DEGs) in this experiment was performed using the DESeq2 package (1.20.0) [45], with an adjusted *p*-value and |log2foldchange| as the threshold for significant differential expression. In particular, the *p*-value was adjusted using Benjamini and Hochberg's method for control of the false discovery rates [46]. The clusterProfiler software was used to perform the Gene Ontology (GO) enrichment analysis of the differential gene sets. To understand the functions of the genes, the Kyoto Encyclopedia of Genes and Genomes (KEGG) (http://www.genome.jp/kegg/ (accessed on 27 July 2022)) was used. Both the GO terms and KEGG with a corrected padj less than 0.05 were considered significantly enriched by the DEGs.

2.6. Validation of DEGs through Quantitative Real-Time Polymerase Chain Reaction (qRT-PCR)

To validate the transcriptomic data, 16 DEGs were selected, and their expression levels were compared in the head samples from viruliferous and non-viruliferous SBPHs using qRT-PCR. The head (without antennae) samples from the viruliferous and non-viruliferous SBPHs were prepared with the same methods described in Section 2.2, and then the RNA was extracted. The cDNA was synthesized using the HiScript®III 1st Strand cDNA Synthesis Kit (+gDNA wiper) (Vazyme, Nanjing, China) following the manufacturer's procedure. A qRT-PCR reaction was performed with the ChamQ^TM SYBR qPCR Master Mix (Vazyme, Nanjing, China), and the specific reaction system and procedure were carried out as previously described [18,47]. The primers were designed by Primer 3 (version 0.4.0, http://bioinfo.ut.ee/primer3-0.4.0/ (accessed on 13 August 2021)) (Table S1). The $2^{-\Delta\Delta CT}$ method was used to calculate the relative expression levels of the target genes [48], and *β-actin* was used as the reference gene [18,42]. Each target gene was performed in three replicates. The data were analyzed and visualized using GraphPad Prism version 8.0.0 (GraphPad Software, San Diego, CA, USA), and Student's *t*-test was used to determine the significance of the relative expression level between the two groups.

3. Results

3.1. Data Quality Evaluation and Mapping to Reference Genome

The transcriptome sequencing of the six libraries constructed from the viruliferous heads (Head_V_1, Head_V_2, and Head_V_3) and non-viruliferous SBPH heads (Head_NV_1, Head_NV_2, and Head_NV_3) and the complete quality evaluation results of the transcriptome data are listed in Table 1. Approximately 41.06 Gb of raw reads were filtered to obtain 40.02 Gb of clean reads, of which 19.79 Gb and 20.23 Gb of clean reads were obtained from the viruliferous and non-viruliferous SBPH heads, respectively. The data quality evaluation revealed that the GC content of each sample exceeded 38.29%, and Q20 and Q30 exceeded 96.38% and 90.89%, respectively, thus indicating that the sequencing data were effective and reliable for use in further analysis. After quality control, the transcriptome sequencing data were mapped to the reference genome (Table 2). The proportion of sequencing reads that were mapped to the genome (Total map) ranged from 61.02 to 65.56%, and the proportion of sequencing reads with a unique alignment position on the reference sequence ranged from 57.3 to 61.53% (Table 2).

Table 1. Summary of the transcriptome sequencing data from the viruliferous and non-viruliferous SBPH heads.

Samples	Raw Reads (Raw Bases)	Clean Reads (Clean Bases)	Q20 (%)	Q30 (%)	GC Content (%)
Head_NV_1	46331750 (6.95G)	45130720 (6.77G)	96.38	90.85	38.29
Head_NV_2	45655372 (6.85G)	44961050 (6.74G)	97.94	93.95	39.93
Head_NV_3	45314050 (6.80G)	44820814 (6.72G)	98.03	94.11	39.27
Head_V_1	43979590 (6.60G)	42331612 (6.35G)	96.5	91.03	39.49
Head_V_2	46100826 (6.92G)	44752470 (6.71G)	96.52	91.04	38.26
Head_V_3	46261636 (6.94G)	44899720 (6.73G)	96.49	91.03	38.78

Table 2. Summary statistics of transcriptome sequencing data mapping to the reference SBPH genome.

Sample	Total Map	Unique Map	Positive Map	Negative Map
Head_NV_1	27538563 (61.02%)	25858563 (57.3%)	12855357 (28.48%)	13003206 (28.81%)
Head_NV_2	29477643 (65.56%)	27663936 (61.53%)	13792682 (30.68%)	13871254 (30.85%)
Head_NV_3	28886428 (64.45%)	27130248 (60.53%)	13533887 (30.2%)	13596361 (30.33%)
Head_V_1	26801186 (63.31%)	25281577 (59.72%)	12598477 (29.76%)	12683100 (29.96%)
Head_V_2	27767897 (62.05%)	26191345 (58.52%)	13049235 (29.16%)	13142110 (29.37%)
Head_V_3	28265984 (62.95%)	26661723 (59.38%)	13278992 (29.57%)	13382731 (29.81%)

3.2. Gene Expression Distribution and Pearson Correlations between Samples

The expected number of fragments per kilobase of transcript sequence per millions of base pairs sequenced (FPKM), is currently the most commonly used method for estimating gene expression levels as it takes into account the effects of the sequencing depth and gene length on the read counts. We calculated the expression values (FPKM) of all genes in each sample and then the boxplot was used to show the distribution of the gene expression levels in different samples. The box plot showed that three respective samples of the head of viruliferous and non-viruliferous SBPHs had similar gene expression distributions (Figure 1). In order to ensure biological repeatability, Pearson's correlation coefficient of the samples within and between the groups was calculated according to the FPKM values of all genes in each sample. A heatmap reflecting Pearson correlations showed that both the non-viruliferous (Head_NV_1, Head_NV_2, and Head_NV_3) and the viruliferous SBPH heads (Head_V_1, Head_V_2, and Head_V_3) were highly correlated within a group, with mean Pearson correlation coefficients above 0.96, while Pearson's correlation coefficients between the two groups were significantly lower than within the group (Figure 2).
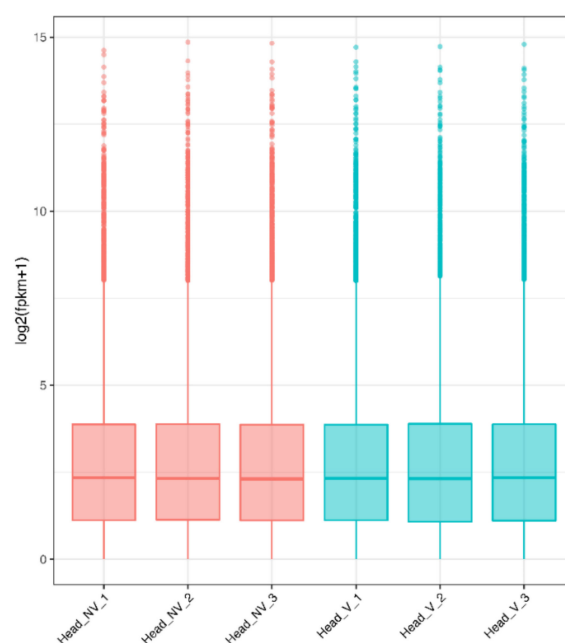
Figure 1. Boxplots of the distribution of gene expression levels (FPKM) for the samples of SBPH; the X-axis represents the names of the samples and the Y-axis represents the log2(FPKM+1).

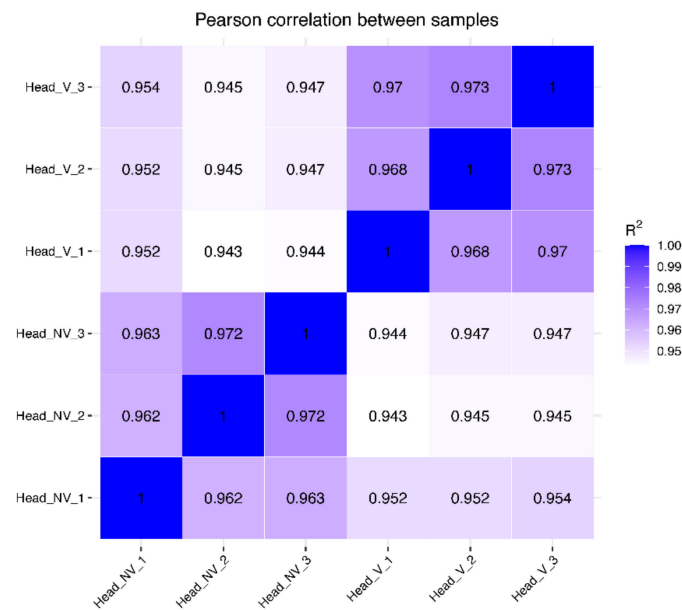**Figure 2.** Pearson correlations of gene expression levels (FPKM) of the six SBPH samples.

3.3. Identification and Analysis of DEGs

The identification of the differentially expressed genes (DEGs) in viruliferous and non-viruliferous SBPH head groups was performed using the DESeq2 package (1.20.0), with the screening conditions of padj (adjusted *p*-value) < 0.05 and |log2foldchange| > 1. The volcano plot and the clustering heat map that displayed the visual expression levels of DEGs between the two groups are clearly shown in Figures 3 and 4, respectively. Compared with the non-viruliferous SBPHs, a total of 336 DEGs were identified in viruliferous SBPH heads, of which 186 genes were up-regulated and 150 genes were down-regulated.
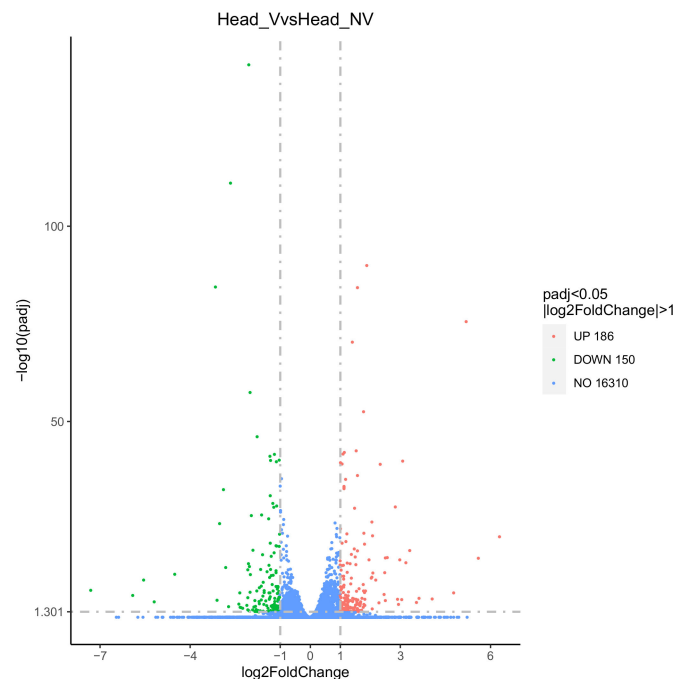

Figure 3. Volcano plot of differentially expressed genes (DEGs) in viruliferous and non-viruliferous SBPH heads; Y-axis represents $-\log_{10}$(padj). Red points indicate up-regulated DEGs, green points indicate down-regulated genes, and blue points indicate genes with no significant difference.
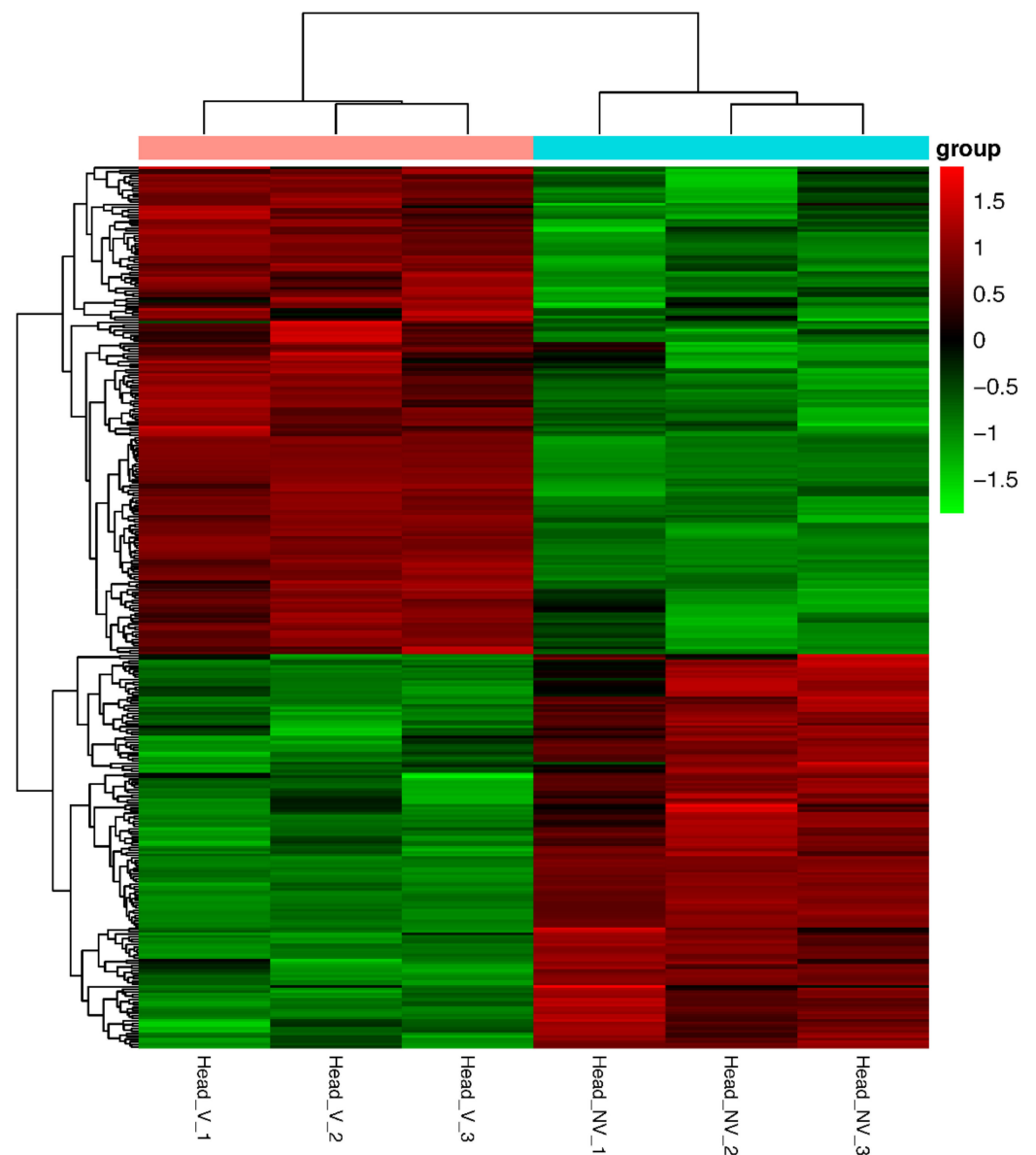
Figure 4. Heat map of differentially expressed genes (DEGs) in viruliferous and non-viruliferous SBPH heads. X-axis represents the names of the samples; Y-axis represents the normalized value of the differential gene FPKM. Red represents higher expression, black represents medium expression, and green represents low expression.

3.4. GO and KEGG Enrichments Analysis of DEGs

GO annotation analysis was conducted to further analyze the functional classification of the DEGs between viruliferous and non-viruliferous heads. The 10 GO subcategories with the highest enrichment in each of the three main GO categories (including molecular function, cellular component, and biological process) were selected, and they are shown in Figure 5. The result showed that the DEGs between viruliferous and non-viruliferous SBPH heads were mainly involved in molecular functions such as endopeptidase activity, peptidase activity, cysteine-type endopeptidase activity, serine-type peptidase activity, serine hydrolase activity, serine-type endopeptidase activity, peptidase activity acting on L-amino acid peptides, and transferase activity transferring one-carbon groups. The enriched biological processes mainly involved the regulation of catalytic activity, the regulation of molecular function, proteolysis, and small-molecule metabolic processes. The GO subcat-

egories of the proton-transporting two-sector ATPase complex, the proton-transporting domain and the extracellular region, were the most abundant in the cellular components.
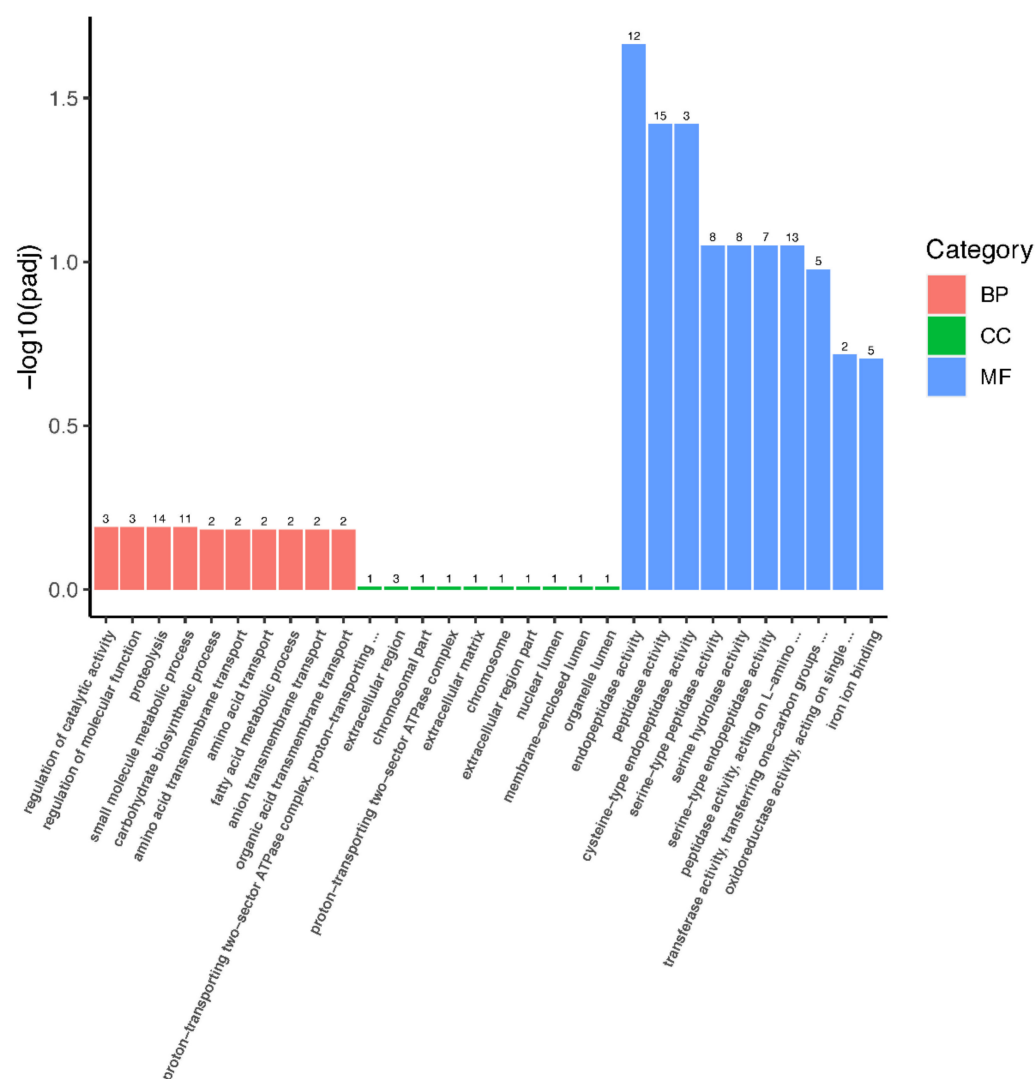

Figure 5. GO enrichment analysis of DEGs in viruliferous and non-viruliferous SBPH heads. X-axis represents GO terms; Y-axis represents the significance level of GO term enrichment. The higher the value, the more significant it is. BP: biological process; CC: cellular component; MF: molecular function.

In order to further analyze the related pathways involved in the DEGs between viruliferous and non-viruliferous SBPH heads, we performed KEGG enrichment analysis, and these DEGs were grouped into 61 biochemical pathways. The top 20 KEGG pathways were selected to draw a scatter plot, and they are displayed as follows (Figure 6), among which the most significant enrichment pathways were related to the lysosome, one-carbon pool by folate, autophagy–animal, glycosaminoglycan degradation, circadian rhythm–fly, other glycan degradation, glycosphingolipid biosynthesis–globo and isoglobo series, glycosylphosphatidylinositol (gpi)–anchor biosynthesis, ascorbate and aldarate metabolism, and amino sugar and nucleotide sugar metabolism. In addition, the neural-related pathway "neuroactive ligand–receptor interaction" was also enriched, with three DEGs aligned to this pathway.
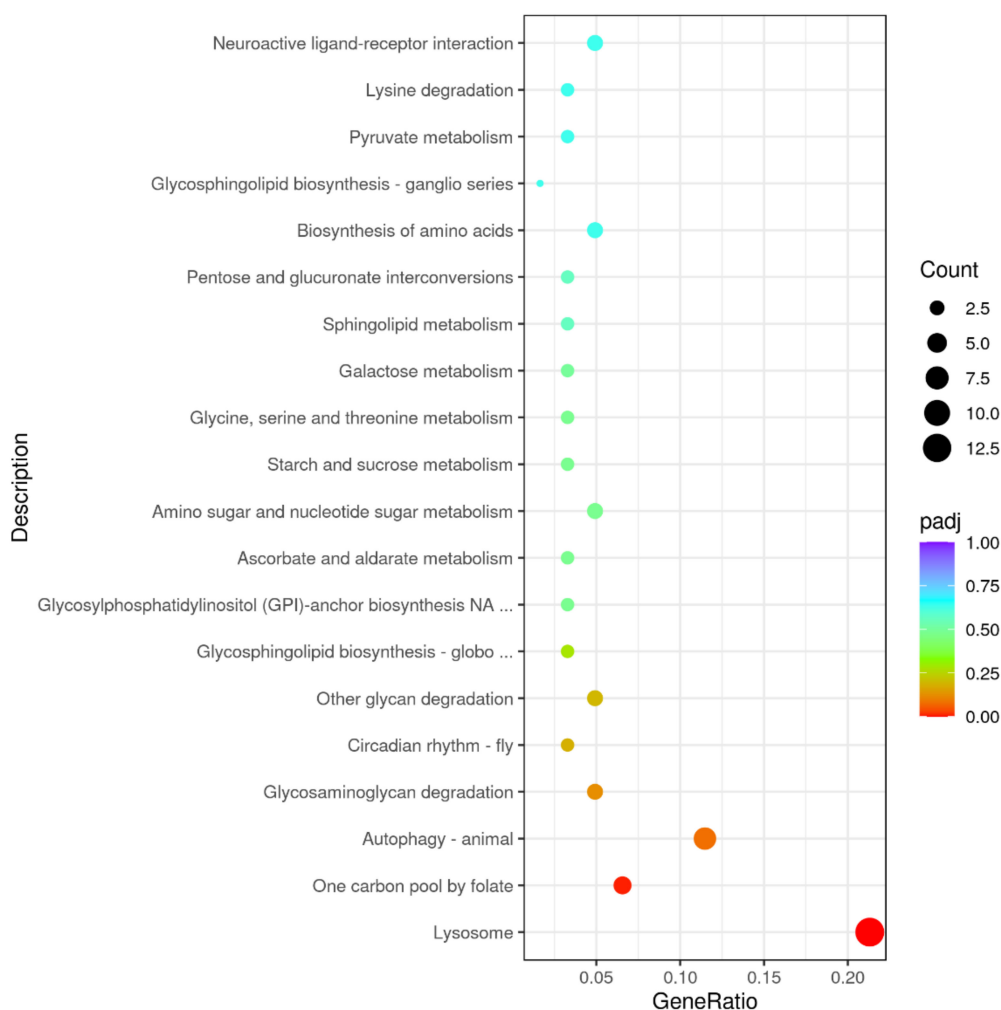
Figure 6. KEGG enrichment analysis of DEGs in viruliferous and non-viruliferous SBPH heads. X-axis represents the ratio of the number of DEGs annotated to the KEGG pathway to the total number of DEGs; Y-axis represents KEGG pathways. The size of the dots represents the number of genes annotated to the KEGG pathway and the padj value ranges from 0 to 1; lower values mean greater intensiveness.

3.5. DEGs Potentially Associated with Virus Transmission

The DEGs possibly associated with virus transmission between viruliferous and non-viruliferous SBPHs were identified, and they are listed in Table 3, including six neural-associated genes, four cytochrome P450s, five sugar-associated genes, four olfaction-related genes, and three cuticular-related genes. Among these genes, most of them had significantly higher expression levels in viruliferous SBPH, except for one neural-associated gene, one cytochrome P450, two sugar-associated genes, and one cuticular-related gene that were significantly diminished. In addition to the above genes, other DEGs potentially involved in regulating RSV transmission were identified, consisting of 10 up-regulated genes, including *E3*, *E74A*, *PLRP2*, and *VgR*, and three down-regulated genes including *period* and *Dsx*.

Table 3. Identification of DEGs possibly associated with virus transmission between viruliferous and non-viruliferous SBPH heads.

Gene ID	Gene Name	Annotation	Length (bp)	p-Value	log$_2$ Fold Change
Neural-associated gene					
LSTR_LSTR006557	EH	eclosion hormone (*Nilaparvata lugens*)	2139	5.91×10^{-18}	5.61
LSTR_LSTR004655	CCH1R	CCHamide-1 receptor (*Nilaparvata lugens*)	1083	0.0015	1.12
LSTR_LSTR005567	FMRFaR	FMRFamide receptor (*Nilaparvata lugens*)	1511	2.73×10^{-10}	1.02
LSTR_LSTR007145	Mth2	G-protein coupled receptor Mth2 (*Nilaparvata lugens*)	1290	1.14×10^{-6}	3.06
LSTR_LSTR012676	5HT$_{1B}$	5-hydroxytryptamine receptor (*Homalodisca vitripennis*)	1562	0.0024	1.03
LSTR_LSTR017186	SK	sulfakinin (*Nilaparvata lugens*)	322	1.03×10^{-13}	−4.50
Cytochrome P450					
LSTR_LSTR014118	CYP6FL1	cytochrome P450 CYP6FL1 (*Sogatella furcifera*)	1677	6.00×10^{-6}	1.28
LSTR_LSTR011334	CBR1	cytochrome b reductase 1 (*Schistocerca gregaria*)	986	2.86×10^{-5}	1.56
LSTR_LSTR004091	CYP314A1	cytochrome P450 CYP314A1, partial (*Laodelphax striatellus*)	3730	4.08×10^{-7}	1.15
LSTR_LSTR000771	CYP4C62	cytochrome P450 CYP4C62 (*Laodelphax striatellus*)	2026	1.17×10^{-115}	−2.64
Sugar-associated gene					
LSTR_LSTR002783	ST4	sugar transporter 4 (*Nilaparvata lugens*)	1998	1.55×10^{-17}	1.97
LSTR_LSTR012604	ST29	sugar transporter 29 (*Nilaparvata lugens*)	3063	1.91×10^{-5}	1.65
LSTR_LSTR010413	ST42	sugar transporter 42 (*Nilaparvata lugens*)	2363	3.22×10^{-10}	1.13
LSTR_LSTR013190	ST27	sugar transporter 27 (*Nilaparvata lugens*)	916	0.0001	−1.81
LSTR_LSTR005915	TPS2	trehalose-6-phosphate synthase 2 (*Nilaparvata lugens*)	3078	2.30×10^{-10}	−1.05

Table 3. *Cont.*

Gene ID	Gene Name	Annotation	Length (bp)	*p*-Value	log$_2$ Fold Change
Olfaction-related gene					
LSTR_LSTR001830	SNMP2	sensory neuron membrane protein 2 (*Nilaparvata lugens*)	942	0.0039	1.13
LSTR_LSTR001538	OR104	odorant receptor 104 (*Halyomorpha halys*)	2015	4.88×10^{-6}	1.57
LSTR_LSTR001409	OR23a	odorant receptor 23a-like (*Nilaparvata lugens*)	1571	0.0022	1.66
LSTR_LSTR007970	OR23a	odorant receptor 23a-like (*Nilaparvata lugens*)	1658	0.0055	1.04
Cuticular-related gene					
LSTR_LSTR005116	CPR61	cuticular protein (*Nilaparvata lugens*)	1713	0.0033	1.40
LSTR_LSTR009161	CPR96	cuticular protein (*Nilaparvata lugens*)	1795	1.23×10^{-9}	1.06
Other virus-transmission-related gene					
LSTR_LSTR011186	ATG13	autophagy-related protein 13 (*Nilaparvata lugens*)	5805	3.49×10^{-31}	1.49
LSTR_LSTR015356	HR38	nuclear hormone receptor HR38 (*Nilaparvata lugens*)	1419	0.0013	−2.07
LSTR_LSTR001348	E3	E3 ubiquitin-protein ligase RNF139 (*Nilaparvata lugens*)	2405	1.10×10^{-16}	1.25
LSTR_LSTR002356	E74A	E74A (*Nilaparvata lugens*)	1203	3.29×10^{-7}	1.05
LSTR_LSTR012920	bicaudal C	protein bicaudal C homolog 1 (*Nilaparvata lugens*)	2890	3.83×10^{-6}	1.23
LSTR_LSTR010541	PLRP2	Pancreatic lipase-related protein 2 (*Nilaparvata lugens*)	3627	7.18×10^{-26}	1.02
LSTR_LSTR011577	VgR	vitellogenin receptor (*Laodelphax striatellus*)	7648	3.40×10^{-14}	1.24
LSTR_LSTR014469	SHP	salivary sheath protein (*Nilaparvata lugens*)	738	4.89×10^{-43}	1.02
LSTR_LSTR003055	HSGC	head-specific guanylate cyclase (*Nilaparvata lugens*)	1894	0.0038	1.01
LSTR_LSTR001253	ApD	apolipoprotein D (*Nilaparvata lugens*)	994	4.60×10^{-9}	1.78
LSTR_LSTR008185	UAP	UDP-N-acetylglucosamine pyrophosphory-lase (*Sogatella furcifera*)	4828	3.81×10^{-11}	1.36

Table 3. *Cont.*

Gene ID	Gene Name	Annotation	Length (bp)	*p*-Value	log$_2$ Fold Change
LSTR_LSTR008501	period	period (*Laodelphax striatellus*)	4424	1.06×10^{-43}	−1.30
LSTR_LSTR016981	U60S	ubiquitin-60S ribosomal protein L40 (*Nilaparvata lugens*)	184	5.15×10^{-6}	−5.18
LSTR_LSTR001934	Dsx	doublesex- and mab-3-related transcription factor 3 (*Nilaparvata lugens*)	2205	1.74×10^{-6}	−1.03

Gene IDs come from the SBPH reference genome [40].

3.6. Transcriptome Validation by qRT-PCR

To validate the reliability of the transcriptome, we investigated 16 selected DEGs associated with virus transmission using qRT-PCR (Figure 7). The expression profiles of these selected DEGs showed a similar trend in transcriptome sequencing, demonstrating the reliability of the transcriptome data. Notably, the relative expression levels of the candidate genes such as *EH*, *CYP4C62*, *ST29*, and *HR38* were up- or down-regulated by more than 100%, which is in high agreement with the corresponding transcriptomic changes. The expressions of *FMRFaR* and *PLRP2* showed an up-regulation exceeding twofold by RSV infection in qRT-PCR results, and less up-regulation in transcriptome sequencing. Interestingly, RSV infection exceeded a 10-fold decrease in *Dsx* expression, which was higher than the transcriptome results. In general, the results revealed that these genes are possibly involved in mediating RSV infection.
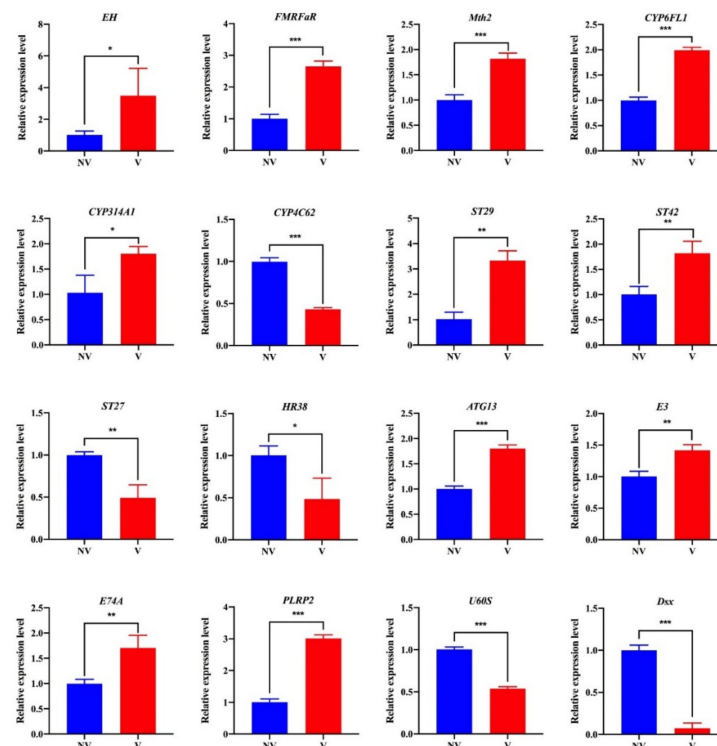

Figure 7. The expression levels of DEGs potentially associated with virus transmission were measured by qRT-PCR. NV represents the heads of non-viruliferous SBPHs, and V represents the heads of viruliferous SBPHs. Student's *t*-test was used to determine the statistical differences between the samples. (* *p* < 0.05, ** *p* < 0.01, *** *p* < 0.001).

4. Discussions

In order to explore the complex interactions between plant viruses and insect vectors, transcriptome sequencing techniques have been applied to many virus–vector systems, including RSV-SBPH [37,41,49,50]. In this study, transcriptome sequencing was used to analyze the transcriptional profiles of SBPH induced by RSV infection. In total, 336 DEGs were identified from viruliferous and non-viruliferous SBPH heads, including 186 up-regulated and 150 down-regulated genes. Overall, sixteen differentially expressed genes were selected for qRT-PCR validation, and the results were consistent with the transcriptomic data. The KEGG enrichment pathways showed that the DEGs related to autophagy–animal, circadian rhythm–fly, amino sugar and nucleotide sugar metabolism, and the neuroactive ligand–receptor interaction were relatively significantly enriched. Meanwhile, further screening analysis of differential genes indicated that most of the DEGs associated with viral infection or transmission were possibly involved in neural-related genes, cytochrome P450 genes, sugar-related genes, olfactory-related genes, and cuticular-related genes. In addition, other DEGs that may be related to virus infection, including autophagy and ubiquitin ligase, were also identified.

The central nervous system (CNS), which mainly exists in the head, plays a vital role in the physiological and behavioral processes of insects. Studies have demonstrated that plant viruses could overcome the transmission barriers and replicate in the CNS of vector insects [51–53]. Interestingly, Wang et al. found that the rice yellow stunt virus (RYSV) matrix protein M interacted with axonal microtubules to promote the continuation of RYSV through its insect vector, *Nephotettix cincticeps*, and observed that the neural factor Hig could interact with the M protein to limit the transmission of RYSV in the CNS [54,55]. Neuropeptides act as neurohormones, neurotransmitters, and neuromodulators and are involved in regulating the physiology and behaviors of insects [56]. In the study, the KEGG enrichments analysis of the DEGs showed that the neuroactive ligand–receptor interaction, a neural-related pathway, was enriched. Four differentially expressed neuropeptide-related genes were identified in this study. *EH*, *CCH1R*, and *FMRFaR* were up-regulated after RSV infection, while *SK* was down-regulated. Similarly, a recent study investigated the transcript levels of neuropeptide genes in the heads of *Spodoptera exigua* larvae infected with *S. exigua* multiple nucleopolyhedrovirus (SeMNPV) and found two up-regulated and seven down-regulated neuropeptide genes [56]. *Mth2* and $5HT_{1B}$ are members of the G-protein-coupled receptor (GPCR) family, which play a crucial role in regulating insect physiology and behavior through the regulation of signaling molecules [57,58], both of which were induced to be up-regulated by RSV infection.

Cytochrome P450 monooxygenases (P450), the most important detoxification enzymes in insects, play critical roles in insect metabolism and development [59,60]. Most of the studies on P450s in insects mainly focused on their roles in insecticide metabolism and resistance [61–64]. In addition, studies have shown that several P450 genes, including CYP314A1, are involved in the synthesis of 20E [65,66]. However, little was known about whether P450s affect virus replication or transmission in insect vectors. Zhang et al. [67] showed that the expressions of 16 P450 genes, including *CYP6CW1* and *CYP6AY3*, changed significantly after RBSDV infection in SBPH, and the transcriptome analysis demonstrated that several P450s changed significantly after virus infection in SBPHs. In this study, most of the differentially expressed P450 genes, including *CYP6FL1*, *CBR1*, and *CYP314A1*, were up-regulated in the heads of the viruliferous SBPHs. The expression of *CYP4C62* was downregulated by RSV infection, which was consistent with the results of RBSDV infection in SBPH [67]. These results indicated that P450 genes might be involved in the interactions between virus and vector insects.

Sugar, an important organic compound that provides energy for organisms, cannot directly pass through the cell membrane, and its transport requires sugar transporters (STs). As the blood glucose of piercing–sucking pests, trehalose plays an important role in growth, development, and stress resistance, and its transmembrane transport depends on the mediation of STs [68]. STs may also be required for the interactions between insects and

pathogens. For example, Sagisaka et al. found that the expressions of sugar transporters were upregulated in *Bombyx mori* infected with nucleopolyhedrovirus [69]. Remarkably, another study found that RSV NP could co-localize with ST6 in the midgut of SBPH, thereby mediating viral entry into midgut epithelial cells, and further experiments showed that the ability of non-viruliferous SBPH to acquire and transmit RSV was significantly reduced after the knockdown of ST6 [23,70]. A total of five sugar-associated DEGs were screened in this study: *ST4*, *ST29*, and *ST42* were up-regulated by RSV infection, while *ST27* and *TPS2* were down-regulated. The results suggested that STs may play a role in the process of RSV infection in SBPH.

The olfactory system of insects is an important chemosensory organ that stimulates the insects to produce corresponding behavioral responses, including odorant-binding proteins (OBPs), chemosensory proteins (CSPs), odorant receptors (ORs)/olfactory co-receptor receptors (ORcos), ionotropic receptors (IR), and sensory neuron membrane proteins (SN-MPs) [71–73]. Many vector-borne viruses can manipulate vector behavior directly or indirectly to facilitate their virus transmission, and this manipulative behavior can be achieved in part by regulating the chemosensory systems of insects, including the olfactory system [41]. OBP2 and OBP3 were involved in regulating the preference of *S. furcifera* and *B. tabaci* to plants with different odor sources (healthy plants or carrying southern rice black-streaked dwarf virus and tomato chlorosis virus), respectively, thereby affecting the spread of viruses [12,13]. In SBPHs, it was found that *Orco* was mainly expressed in the heads of SBPHs, and RSV infection could significantly stimulate its expression [74]. In this study, four DEGs in the olfactory system, including *SNMP2*, *OR104*, and *OR23a*, were screened, and they were all induced to increase in the heads of SBPHs after RSV infection. These results are consistent with the study that suggested that RSV infection upregulated the expressions of *OBP2* and *SNMP2-2* [41].

Cuticular proteins are important structural proteins in insects, playing an important role in physiological and behavioral processes such as insect growth, reproduction, and environmental adaptation [75]. In addition, cuticular proteins in the stylets of *M. persicae* that transmits Zucchini yellow mosaic virus [76], *Schizaphis graminum* that transmits Cereal yellow dwarf virus [77], and *Brevicoryne brassicae* that transmits cauliflower mosaic virus [78] could interact with the virus proteins, respectively, thus affecting the transmission of plant viruses. In SBPHs, Liu et al. found that cuticular protein, CPR1, could co-localize with RSV in the hemolymph of SBPHs. Further experiments showed that the knockdown of CPR1 reduced the content of the virus in the hemolymph and salivary glands, as well as the horizontal transmission rate, indicating that CPR1 plays a key role in virus transmission [24]. In this study, two cuticular proteins, *CPR61* and *CPR96*, were induced after RSV infection, indicating that there may be other cuticular proteins other than CPR1 that function in RSV infection.

VgR-mediated endocytosis is essential for RSV to bind to Vg and enter the germarium nurse cell, thereby completing vertical transmission in SBPHs [20,79]. Transcriptome studies on the ovaries of viruliferous and non-viruliferous SBPHs showed that *VgR* was significantly highly expressed in the ovaries of viruliferous SBPHs, and that silencing its expression reduced the titer of RSV in the SBPH ovaries significantly [20,80]. Correspondingly, the transcriptome results showed that the expression level of *VgR* in viruliferous SBPH heads was significantly higher than that in non-viruliferous heads, indicating the important role of VgR in RSV transmission. Transcription factor E74 is one of the early ecdysone response genes, which has two alternative splicing isoforms (E74A and E74B) [81]. The research performed by Sun et al. [82] showed that *E74A* could regulate the Vg transcription, and this gene was induced and up-regulated by RSV in SBPHs.

Autophagy is a process of the innate cellular immune response through cellular degradation, and its regulatory role in plant-virus–vector insect systems usually requires the participation of autophagy-related genes (ATGs) [83,84]. A recent study has shown that SRBSDV infection activated the expression of autophagy-related genes *ATG3* and *ATG9* in *S. furcifera*, and the silencing of these two genes promoted the propagation and

transmission of SRBSDV [84]. Unusually, although the autophagic activity of SBPH did not directly affect RSV transmission, it promoted RSV reproduction and transmission by increasing the phosphorylation of c-Jun N-terminal kinase, the virus promotion that may be activated by ATG8 in an autophagy-independent manner [26,31]. Here, the DEG related to autophagy was *ATG13*, which was significantly highly expressed in viruliferous SBPHs. We speculated that ATG13 might also be involved in the regulation of RSV infection and transmission, and the underlying mechanism requires further study.

The ubiquitin–proteasome system (UPS) is a ubiquitous protein-selective degradation system in eukaryotic cells and plays an important role in almost all cellular processes. Protein ubiquitination requires a series of enzymes including ubiquitin-activating enzyme (E1), ubiquitin-conjugating enzyme (E2), and ubiquitin ligase (E3) [85,86]. Li et al. showed that RSV induced the expression of *E2-E* in SBPHs, and E2-E, which might inhibit the accumulation of RSV through unknown antiviral mechanisms [27]. The RSV-induced *E3* expression in this study may further support the author's conjecture that E2-E catalyzes the ubiquitination and degradation of the virus under the catalysis of E3 to inhibit the replication and the accumulation of the virus [27]. Remarkably, transcription factor *Dsx* involved in sex determination in SBPHs was significantly down-regulated after RSV infection. The potential mechanism for the down-regulation and the role of the gene in the virus–vector relationship deserves further study.

5. Conclusions

In summary, transcriptome sequencing revealed that RSV infection changed the gene expressions in the heads of SBPHs. The DEGs identified in this study belonged to different molecular and/or cellular pathways with possible implications for RSV transmission and replication in SBPH. The results in the current study are similar to the previous studies that reported transcriptomic responses of SBPH from the midgut, whole body, and other organs/tissues [30,35–37,40,41], signifying that infection of RSV in SBPH leads to similarly altered global gene expression profiles. In addition, the current study identified some interesting DEGs in nervous systems (EH, CCH1R, FMRFaR, SK, Mth2, and $5HT_{1B}$). As the nervous system controls the insect life cycle, differential expression of these genes in viruliferous SBPH opens a new opportunity to test the effects of these genes on SBPH biology and behavior.

References

1. Eigenbrode, S.D.; Bosque-Pérez, N.A.; Davis, T.S. Insect-Borne plant pathogens and their vectors: Ecology, evolution, and complex interactions. *Annu. Rev. Entomol.* **2018**, *63*, 169–191. [CrossRef] [PubMed]
2. Verheggen, F.; Barrès, B.; Bonafos, R.; Desneux, N.; Escobar-Gutiérrez, A.J.; Gachet, E.; Laville, J.; Siegwart, M.; Thiéry, D.; Jactel, H. Producing sugar beets without neonicotinoids: An evaluation of alternatives for the management of viruses-transmitting aphids. *Entomol. Gen.* **2022**, *42*, 491–498. [CrossRef]
3. Moreno, A.; Miranda, M.P.; Fereres, A. Psyllids as major vectors of plant pathogens. *Entomol. Gen.* **2021**, *41*, 419–438. [CrossRef]

4. LoTora, A.G.; Lai, P.C.; Chen, Y.J.; Gautam, S.; Abney, M.R.; Srinivasan, R. *Frankliniella fusca* (Thysanoptera: Thripidae), the vector of *tomato spotted wilt orthotospovirus* infecting peanut in the southeastern united states. *J. Integr. Pest Manag.* **2022**, *13*, 3. [CrossRef]

5. Bodino, N.; Cavalieri, V.; Pegoraro, M.; Altamura, G.; Canuto, F.; Zicca, S.; Fumarola, G.; Almeida, R.P.P.; Saponari, M.; Dongiovanni, C. Temporal dynamics of the transmission of *Xylella fastidiosa* subsp. pauca by *Philaenus spumarius* to olive plants. *Entomol. Gen.* **2021**, *41*, 463–480. [CrossRef]

6. Mauck, K.E.; De Moraes, C.M.; Mescher, M.C. Deceptive chemical signals induced by a plant virus attract insect vectors to inferior hosts. *Proc. Natl. Acad. Sci. USA* **2010**, *107*, 3600–3605. [CrossRef]

7. Keesey, I.W.; Koerte, S.; Khallaf, M.A.; Retzke, T.; Guillou, A.; Grosse-Wilde, E.; Buchon, N.; Knaden, M.; Hansson, B.S. Pathogenic bacteria enhance dispersal through alteration of *Drosophila* social communication. *Nat. Commun.* **2017**, *8*, 265. [CrossRef]

8. Gautam, S.; Gadhave, K.R.; Buck, J.W.; Dutta, B.; Coolong, T.; Adkins, S.; Srinivasan, R. Virus-virus interactions in a plant host and in a hemipteran vector: Implications for vector fitness and virus epidemics. *Virus Res.* **2020**, *286*, 198069. [CrossRef]

9. Gautam, S.; Mugerwa, H.; Sundaraj, S.; Gadhave, K.R.; Murphy, J.F.; Dutta, B.; Srinivasan, R. Specific and spillover effects on vectors following infection of two RNA viruses in pepper plants. *Insects* **2020**, *11*, 602. [CrossRef]

10. Ngumbi, E.; Eigenbrode, S.D.; Bosque-Pérez, N.A.; Ding, H.; Rodriguez, A. *Myzus persicae* is arrested more by blends than by individual compounds elevated in headspace of plrv-infected potato. *J. Chem. Ecol.* **2007**, *33*, 1733–1747. [CrossRef]

11. Wang, S.; Guo, H.; Ge, F.; Sun, Y. Apoptotic neurodegeneration in whitefly promotes the spread of TYLCV. *eLife* **2020**, *9*, e56168. [CrossRef]

12. Shi, X.B.; Wang, X.Z.; Zhang, D.Y.; Zhang, Z.H.; Zhang, Z.; Cheng, J.; Zheng, L.M.; Zhou, X.G.; Tan, X.Q.; Liu, Y. Silencing of odorant-binding protein gene *OBP3* using RNA interference reduced virus transmission of tomato chlorosis virus. *Int. J. Mol. Sci.* **2019**, *20*, 4969. [CrossRef]

13. Hu, K.; Yang, H.H.; Liu, S.; He, H.L.; Ding, W.B.; Qiu, L.; Li, Y.Z. Odorant-binding protein 2 is involved in the preference of *Sogatella furcifera* (Hemiptera: Delphacidae) for rice plants infected with the southern rice black-streaked dwarf virus. *Fla. Entomol.* **2019**, *102*, 353. [CrossRef]

14. Fang, Y.; Choi, J.Y.; Park, D.H.; Park, M.G.; Kim, J.Y.; Wang, M.; Kim, H.J.; Kim, W.J.; Je, Y.H. Suppression of rice stripe virus replication in *Laodelphax striatellus* using vector insect-derived double-stranded RNAs. *Plant Pathol. J.* **2020**, *36*, 280–288. [CrossRef]

15. Fang, Y.; Park, M.G.; Choi, J.Y.; Park, D.H.; Wang, M.; Kim, H.J.; Kim, W.J.; Je, Y.H. Insecticidal and synergistic activity of dsRNAs targeting buprofezin-specific genes against the small brown planthopper, *Laodelphax striatellus*. *Arch. Insect Biochem. Physiol.* **2020**, *105*, e21739. [CrossRef]

16. An, S.B.; Choi, J.Y.; Lee, S.H.; Fang, Y.; Kim, J.H.; Park, D.H.; Park, M.G.; Woo, R.M.; Kim, W.J.; Je, Y.H. Silencing of rice stripe virus in *Laodelphax striatellus* using virus-derived double-stranded RNAs. *J. Asia-Pac. Entomol.* **2017**, *20*, 695–698. [CrossRef]

17. Xu, Y.; Fu, S.; Tao, X.; Zhou, X. *Rice stripe virus*: Exploring molecular weapons in the arsenal of a negative-sense RNA virus. *Annu. Rev. Phytopathol.* **2021**, *59*, 351–371. [CrossRef]

18. Zhang, Y.Y.; Xu, G.; Jiang, Y.; Ma, C.; Yang, G.Q. Sublethal effects of imidacloprid on fecundity, apoptosis and virus transmission in the small brown planthopper *Laodelphax striatellus*. *Insects* **2021**, *12*, 1131. [CrossRef]

19. Huo, Y.; Yu, Y.L.; Chen, L.Y.; Li, Q.; Zhang, M.T.; Song, Z.Y.; Chen, X.Y.; Fang, R.X.; Zhang, L.L. Insect tissue-specific vitellogenin facilitates transmission of plant virus. *PLoS Pathog.* **2018**, *14*, e1006909. [CrossRef]

20. Huo, Y.; Yu, Y.L.; Liu, Q.; Liu, D.; Zhang, M.T.; Liang, J.N.; Chen, X.Y.; Zhang, L.L.; Fang, R.X. Rice stripe virus hitchhikes the vector insect vitellogenin ligand-receptor pathway for ovary entry. *Philos. Trans. R. Soc. B* **2019**, *374*, 20180312.

21. Li, Y.; Chen, D.Y.; Hu, J.; Zhang, K.; Kang, L.; Chen, Y.; Huang, L.J.; Zhang, L.; Xiang, Y.; Song, Q.S.; et al. The α-tubulin of *Laodelphax striatellus* mediates the passage of rice stripe virus (RSV) and enhances horizontal transmission. *PLoS Pathog.* **2020**, *16*, e1008710. [CrossRef] [PubMed]

22. Ma, Y.H.; Lu, H.; Wang, W.; Zhu, J.M.; Zhao, W.; Cui, F. Membrane association of importin α facilitates viral entry into salivary gland cells of vector insects. *Proc. Natl. Acad. Sci. USA* **2021**, *118*, e2103393118. [CrossRef] [PubMed]

23. Qin, F.L.; Liu, W.W.; Wu, N.; Zhang, L.; Zhang, Z.K.; Zhou, X.P.; Wang, X.F. Invasion of midgut epithelial cells by a persistently transmitted virus is mediated by sugar transporter 6 in its insect vector. *PLoS Pathog.* **2018**, *14*, e1007201. [CrossRef] [PubMed]

24. Liu, W.W.; Gray, S.W.; Huo, Y.; Li, L.; Wei, T.Y.; Wang, X.F. Proteomic analysis of interaction between a plant virus and its vector insect reveals new functions of Hemipteran cuticular protein. *Mol. Cell. Proteom.* **2015**, *14*, 2229–2242. [CrossRef] [PubMed]

25. Xu, Y.; Wu, J.X.; Fu, S.; Li, C.Y.; Zhu, Z.R.; Zhou, X.P. Rice stripe tenuivirus nonstructural protein 3 hijacks the 26S proteasome of the small brown planthopper via direct interaction with regulatory particle non-ATPase subunit 3. *J. Virol.* **2015**, *89*, 4296–4310. [CrossRef]

26. Wang, W.; Zhao, W.; Li, J.; Luo, L.; Kang, L.; Cui, F. The c-Jun N-terminal kinase pathway of a vector insect is activated by virus capsid protein and promotes viral replication. *eLife* **2017**, *6*, e26591. [CrossRef]

27. Li, Y.; Zhou, Z.; Shen, M.; Ge, L.Q.; Liu, F. Ubiquitin-conjugating enzyme E2 E inhibits the accumulation of rice stripe virus in *Laodelphax striatellus* (Fallén). *Viruses* **2020**, *12*, 908. [CrossRef]

28. Fang, Y.; Choi, J.Y.; Lee, S.H.; Kim, J.H.; Park, D.H.; Park, M.G.; Woo, R.M.; Lee, B.R.; Kim, W.J.; Li, S.; et al. RNA interference of E75 nuclear receptor gene suppresses transmission of rice stripe virus in *Laodelphax striatellus*. *J. Asia-Pac. Entomol.* **2017**, *20*, 1140–1144. [CrossRef]

29. Li, S.; Li, X.; Zhou, Y.J. Ribosomal protein L18 is an essential factor that promote rice stripe virus accumulation in small brown planthopper. *Virus Res.* **2018**, *247*, 15–20. [CrossRef]

30. Huang, H.J.; Yan, X.T.; Wang, X.; Qi, Y.H.; Lu, G.; Chen, J.P.; Zhang, C.X.; Li, J.M. Proteomic analysis of *Laodelphax striatellus* in response to rice stripe virus infection reveal a potential role of ZFP36L1 in restriction of viral proliferation. *J. Proteom.* **2021**, *239*, 104–184. [CrossRef]

31. Yu, Y.L.; Zhang, M.T.; Huo, Y.; Tang, J.L.; Liu, Q.; Chen, X.Y.; Fang, R.X.; Zhang, L.L. *Laodelphax striatellus* Atg8 facilitates rice stripe virus infection in an autophagy-independent manner. *Insect Sci.* **2021**, *28*, 315–329. [CrossRef]

32. Li, J.; Pan, W.Y.; Zhao, S.L.; Liang, C.Y. Heat shock cognate protein 70 is required for rice stripe tenuivirus accumulation and transmission in small brown planthopper. *Arch. Virol.* **2022**, *167*, 839–848. [CrossRef]

33. Huo, Y.; Song, Z.Y.; Wang, H.T.; Zhang, Z.Y.; Xiao, N.; Fang, R.X.; Zhang, Y.M.; Zhang, L.L. GrpE is involved in mitochondrial function and is an effective target for RNAi-mediated pest and arbovirus control. *Insect Mol. Biol.* **2022**, *31*, 377–390. [CrossRef]

34. Wang, X.; Xu, X.; Ullah, F.; Ding, Q.; Gao, X.W.; Desneux, N.; Song, D. Comparison of full-length transcriptomes of different imidacloprid-resistant strains of *Rhopalosiphum padi* (L.). *Entomol. Gen.* **2021**, *41*, 289–304. [CrossRef]

35. Zhang, Z.; Zhang, P.; Li, W.; Zhang, J.; Huang, F.; Yang, J.; Bei, Y.; Lu, Y. De novo transcriptome sequencing in *Frankliniella occidentalis* to identify genes involved in plant virus transmission and insecticide resistance. *Genomics* **2013**, *101*, 296–305. [CrossRef]

36. Lee, J.H.; Choi, J.Y.; Tao, X.Y.; Kim, J.S.; Kim, W.; Je, Y.H. Transcriptome analysis of the small brown planthopper, *Laodelphax Striatellus* carrying rice stripe virus. *Plant Pathol. J.* **2013**, *29*, 330–337. [CrossRef]

37. Zhao, W.; Lu, L.; Yang, P.; Cui, N.; Kang, L.; Cui, F. Organ-specific transcriptome response of the small brown planthopper toward rice stripe virus. *Insect Biochem. Mol. Biol.* **2016**, *70*, 60–72. [CrossRef]

38. Mugerwa, H.; Gautam, S.; Catto, M.A.; Dutta, B.; Brown, J.K.; Adkins, S.; Srinivasan, R. Differential transcriptional responses in two old world *Bemisia tabaci* cryptic species post acquisition of old and new world begomoviruses. *Cells* **2022**, *11*, 2060. [CrossRef]

39. Catto, M.A.; Mugerwa, H.; Myers, B.K.; Pandey, S.; Dutta, B.; Srinivasan, R. A review on transcriptional responses of interactions between insect vectors and plant viruses. *Cells* **2022**, *11*, 693. [CrossRef]

40. Zhu, J.; Jiang, F.; Wang, X.; Yang, P.; Bao, Y.; Zhao, W.; Wang, W.; Lu, H.; Wang, Q.; Cui, N. Genome sequence of the small brown planthopper, *Laodelphax Striatellus*. *Gigascience* **2017**, *6*, gix109. [CrossRef]

41. Li, Y.; Zhang, Y.; Xiang, Y.; Chen, D.; Hu, J.; Liu, F. Comparative transcriptome analysis of chemoreception organs of *Laodelphax striatellus* in response to rice stripe virus infection. *Int. J. Mol. Sci.* **2021**, *22*, 10299. [CrossRef] [PubMed]

42. Xu, G.; Jiang, Y.; Zhang, N.N.; Liu, F.; Yang, G.Q. Triazophos-induced vertical transmission of rice stripe virus is associated with host vitellogenin in the small brown planthopper *Laodelphax striatellus*. *Pest Manag. Sci.* **2020**, *76*, 1949–1957. [CrossRef] [PubMed]

43. Shah, A.Z.; Ma, C.; Zhang, Y.; Zhang, Q.; Xu, G.; Yang, G. Decoyinine induced resistance in rice against small brown planthopper *Laodelphax striatellus*. *Insects* **2022**, *13*, 104. [CrossRef] [PubMed]

44. Wang, G.Z.; Zhou, Y.J.; Chen, Z.X.; Zhou, X.P. Production of monoclonal antibodies to rice stripe virus and application in virus detection. *Acta Phytopathol. Sin.* **2004**, *34*, 302–306.

45. Anders, S.; Huber, W. Differential expression analysis for sequence count data. *Genome Biol.* **2010**, *11*, R106. [CrossRef]

46. Ferreira, J.A. The Benjamini-Hochberg method in the case of discrete test statistics. *Int. J. Biostat.* **2007**, *3*, 11. [CrossRef]

47. Ma, C.; Zhang, Y.Y.; Gui, W.; Zhang, Q.X.; Xu, G.; Yang, G.Q. Priming of rice seed with decoyinine enhances resistance against the brown planthopper *Nilparvata lugens*. *Crop Prot.* **2022**, *157*, 105970. [CrossRef]

48. Livak, K.J.; Schmittgen, T.D. Analysis of relative gene expression data using real-time quantitative PCR and the $2^{-\Delta\Delta CT}$ method. *Methods* **2001**, *25*, 402–408. [CrossRef]

49. Kaur, N.; Hasegawa, D.K.; Ling, K.S.; Wintermantel, W.M. Application of genomics for understanding plant virus-insect vector interactions and insect vector control. *Phytopathology* **2016**, *106*, 1213–1222. [CrossRef]

50. Zhang, F.; Guo, H.; Zheng, H.; Zhou, T.; Zhou, Y.; Wang, S.; Fang, R.; Qian, W.; Chen, X. Massively parallel pyrosequencing-based transcriptome analyses of small brown planthopper (*Laodelphax striatellus*), a vector insect transmitting rice stripe virus (RSV). *BMC Genom.* **2010**, *11*, 303. [CrossRef]

51. Ammar, E.D.; Hogenhout, S.A. A neurotropic route for maize mosaic virus (Rhabdoviridae) in its planthopper vector *Peregrinus maidis*. *Virus Res.* **2008**, *131*, 77–85. [CrossRef]

52. Whitfield, A.E.; Huot, O.B.; Martin, K.M.; Kondo, H.; Dietzgen, R.G. Plant rhabdoviruses-their origins and vector interactions. *Curr. Opin. Virol.* **2018**, *33*, 198–207. [CrossRef]

53. Zhao, P.; Sun, X.; Li, P.; Sun, J.; Yue, Y.; Wei, J.; Wei, T.; Jia, D. Infection characteristics of rice stripe mosaic virus in the body of the vector leafhoppers. *Front. Microbiol.* **2019**, *9*, 3258. [CrossRef]

54. Wang, H.; Wang, J.; Zhang, Q.; Zeng, T.; Zheng, Y.; Chen, H.; Zhang, X.F.; Wei, T. Rice yellow stunt nucleorhabdovirus matrix protein mediates viral axonal transport in the central nervous system of its insect vector. *Front. Microbiol.* **2019**, *10*, 939. [CrossRef]

55. Wang, H.; Liu, Y.; Mo, L.; Huo, C.; Wang, Z.; Zhong, P.; Jia, D.; Zhang, X.; Chen, Q.; Chen, H.; et al. A neuron-specific antiviral mechanism modulates the persistent infection of rice rhabdoviruses in leafhopper vectors. *Front. Microbiol.* **2020**, *11*, 513. [CrossRef]

56. Llopis-Giménez, A.; Parenti, S.; Han, Y.; Ros, V.I.D.; Herrero, S. A proctolin-like peptide is regulated after baculovirus infection and mediates in caterpillar locomotion and digestion. *Insect Sci.* **2021**, *29*, 230–244. [CrossRef]

57. Ja, W.W.; West, A.P., Jr.; Delker, S.L.; Bjorkman, P.J.; Benzer, S.; Roberts, R.W. Extension of *Drosophila melanogaster* life span with a GPCR peptide inhibitor. *Nat. Chem. Biol.* **2007**, *3*, 415–419. [CrossRef]

58. Watanabe, T.; Sadamoto, H.; Aonuma, H. Identification and expression analysis of the genes involved in serotonin biosynthesis and transduction in the field cricket *Gryllus bimaculatus*. *Insect Mol. Biol.* **2011**, *20*, 619–635. [CrossRef]

59. Xu, D.D.; Liao, H.J.; Li, L.Y.; Wu, M.M.; Xie, W.; Wu, Q.J.; Zhang, Y.J.; Zhou, X.M.; Wang, S.L. The CYP392D8 gene is not directly associated with abamectin resistance, a case study in two highly resistant *Tetranychus urticae* strains. *Entomol. Gen.* **2022**. *published online*. [CrossRef]

60. Zhang, Y.; Feng, Z.J.; Chen, Z.S.; Wang, X.X.; Cong, H.S.; Fan, Y.L.; Liu, T.X. Connection between cuticular hydrocarbons and melanization in *Harmonia axyridis* revealed by RNAi-mediated silencing of the CYP4G79. *Entomol. Gen.* **2021**, *41*, 83–96. [CrossRef]

61. Zhang, Y.; Yang, Y.; Sun, H.; Liu, Z. Metabolic imidacloprid resistance in the brown planthopper, *Nilaparvata lugens*, relies on multiple P450 enzymes. *Insect Biochem. Mol. Biol.* **2016**, *79*, 50–56. [CrossRef] [PubMed]

62. Zhang, Y.; Han, Y.; Liu, B.; Yang, Q.; Guo, H.; Liu, Z.; Wang, L.; Fang, J. Resistance monitoring and cross-resistance role of CYP6CW1 between buprofezin and pymetrozine in field populations of *Laodelphax striatellus* (Fallén). *Sci. Rep.* **2017**, *7*, 14639. [CrossRef] [PubMed]

63. Zhang, J.; Zhang, Y.; Wang, Y.; Yang, Y.; Cang, X.; Liu, Z. Expression induction of P450 genes by imidacloprid in *Nilaparvata lugens*: A genome-scale analysis. *Pestic. Biochem. Physiol.* **2016**, *132*, 59–64. [CrossRef] [PubMed]

64. Xu, L.; Wu, M.; Han, Z. Overexpression of multiple detoxification genes in deltamethrin resistant *Laodelphax striatellus* (Hemiptera: Delphacidae) in China. *PLoS ONE* **2013**, *8*, e79443. [CrossRef] [PubMed]

65. Niwa, R.; Niwa, Y.S. Enzymes for ecdysteroid biosynthesis: Their biological functions in insects and beyond. *Biosci. Biotechnol. Biochem.* **2014**, *78*, 1283–1292. [CrossRef]

66. Iga, M.; Kataoka, H. Recent studies on insect hormone metabolic pathways mediated by cytochrome P450 enzymes. *Biol. Pharm. Bull.* **2012**, *35*, 838–843. [CrossRef]

67. Zhang, J.H.; Zhao, M.; Zhou, Y.J.; Xu, Q.F.; Yang, Y.X. Cytochrome P450 Monooxygenases CYP6AY3 and CYP6CW1 regulate rice black-streaked dwarf virus replication in *Laodelphax striatellus* (Fallén). *Viruses* **2021**, *13*, 1576. [CrossRef]

68. Kikawada, T.; Saito, A.; Kanamori, Y.; Nakahara, Y.; Iwata, K.; Tanaka, D.; Watanabe, M.; Okuda, T. Trehalose transporter 1, a facilitated and high-capacity trehalose transporter, allows exogenous trehalose uptake into cells. *Proc. Natl. Acad. Sci. USA* **2007**, *104*, 11585–11590. [CrossRef]

69. Sagisaka, A.; Fujita, K.; Nakamura, Y.; Ishibashi, J.; Noda, H.; Imanishi, S.; Mita, K.; Yamakawa, M.; Tanaka, H. Genome-wide analysis of host gene expression in the silkworm cells infected with *Bombyx mori* nucleopolyhedrovirus. *Virus Res.* **2010**, *147*, 166–175. [CrossRef]

70. Hajano, J.; Raza, A.; Zhang, L.; Liu, W.; Wang, X. Ribavirin targets sugar transporter 6 to suppress acquisition and transmission of rice stripe tenuivirus by its vector *Laodelphax striatellus*. *Pest Manag. Sci.* **2020**, *76*, 4086–4092. [CrossRef]

71. Leal, S.W. Odorant reception in insects: Roles of receptors, binding proteins, and degrading enzymes. Annu. *Rev. Entomol.* **2013**, *58*, 373–391. [CrossRef]

72. Pelosi, P.; Iovinella, I.; Zhu, J.; Wang, G.; Dani, F.R. Beyond chemoreception: Diverse tasks of soluble olfactory proteins in insects. *Biol. Rev.* **2018**, *93*, 184–200. [CrossRef]

73. Grapputo, A.; Thrimawithana, A.H.; Steinwender, B.; Newcomb, R.D. Differential gene expression in the evolution of sex pheromone communication in New Zealand's endemic leafroller moths of the genera *Ctenopseustis* and *Planotortrix*. *BMC Genom.* **2018**, *19*, 94. [CrossRef]

74. Li, S.; Zhou, C.; Zhou, Y. Olfactory co-receptor Orco stimulated by Rice stripe virus is essential for host seeking behavior in small brown planthopper. *Pest Manag. Sci.* **2018**, *75*, 187–194. [CrossRef]

75. Futahashi, R.; Okamoto, S.; Kawasaki, H.; Zhong, Y.S.; Iwanaga, M.; Mita, K.; Fujiwara, H. Genome-wide identification of cuticular protein genes in the silkworm, *Bombyx mori*. *Insect Biochem. Mol. Biol.* **2008**, *38*, 1138–1146. [CrossRef]

76. Dombrovsky, A.; Gollop, N.; Chen, S.; Chejanovsky, N.; Raccah, B. In vitro association between the helper component-proteinase of zucchini yellow mosaic virus and cuticle proteins of *Myzus persicae*. *J. Gen. Virol.* **2007**, *88*, 1602–1610. [CrossRef]

77. Cilia, M.; Tamborindeguy, C.; Fish, T.; Howe, K.; Thannhauser, T.W.; Gray, S. Genetics coupled to quantitative intact proteomics links heritable aphid and endosymbiont protein expression to circulative polerovirus transmission. *J. Virol.* **2011**, *85*, 2148–2166. [CrossRef]

78. Uzest, M.; Gargani, D.; Drucker, M.; Hébrard, E.; Garzo, E.; Candresse, T.; Fereres, A.; Blanc, S. A protein key to plant virus transmission at the tip of the insect vector stylet. *Proc. Natl. Acad. Sci. USA* **2007**, *104*, 17959–17964. [CrossRef]

79. Huo, Y.; Liu, W.; Zhang, F.; Chen, X.; Li, L.; Liu, Q.; Zhou, Y.; Wei, T.; Fang, R.; Wang, X. Transovarial transmission of a plant virus is mediated by vitellogenin of its insect vector. *PLoS Pathog.* **2014**, *10*, e1003949. [CrossRef]

80. He, K.; Lin, K.; Ding, S.; Wang, G.; Li, F. The vitellogenin receptor has an essential role in vertical transmission of rice stripe virus during oogenesis in the small brown plant hopper. *Pest Manag. Sci.* **2018**, *75*, 1370–1382. [CrossRef]

81. Stilwell, G.E.; Nelson, C.A.; Weller, J.; Cui, H.; Hiruma, K.; Truman, J.W.; Riddiford, L.M. E74 exhibits stage-specific hormonal regulation in the epidermis of the tobacco hornworm, *Manduca Sexta*. *Dev. Biol.* **2003**, *258*, 76–90. [CrossRef] [PubMed]

82. Sun, Z.; Shi, Q.; Xu, C.; Wang, R.; Wang, H.; Song, Y.; Zeng, R. Regulation of NlE74A on vitellogenin may be mediated by angiotensin converting enzyme through a fecundity-related SNP in the brown planthopper, *Nilaparvata lugens*. *Comp. Biochem. Physiol. Part A Mol. Integr. Physiol.* **2018**, *225*, 26–32. [CrossRef] [PubMed]

83. Shelly, S.; Lukinova, N.; Bambina, S.; Berman, A.; Cherry, S. Autophagy is an essential component of *Drosophila* immunity against vesicular stomatitis virus. *Immunity* **2009**, *30*, 588–598. [CrossRef] [PubMed]

84. Liu, D.; Li, Z.; Hou, M. Silencing the autophagy-related genes ATG3 and ATG9 promotes SRBSDV propagation and transmission in *Sogatella furcifera*. *Insects* **2022**, *13*, 394. [CrossRef]

85. Swatek, K.N.; Komander, D. Ubiquitin modifications. *Cell Res.* **2016**, *26*, 399–422. [CrossRef]

86. Patterson, C. Search and destroy: The role of protein quality control in maintaining cardiac function. *J. Mol. Cell. Cardiol.* **2006**, *40*, 438–441. [CrossRef]